

AMARSI: AEROSOL MODELING AND RETRIEVAL FROM MULTI-SPECTRAL IMAGERS

G. de Leeuw^(1,2,3), R.L. Currier⁽¹⁾, A. Staroverova⁽²⁾, A. Kokhanovsky⁽⁴⁾, W. Von Hoyningen-Huene⁽⁴⁾, V.V. Rozanov⁽⁴⁾, J.P. Burrows⁽⁴⁾, G. Hesselmann⁽⁵⁾, L. Gale⁽⁵⁾ and M. Bouvet⁽⁶⁾

⁽¹⁾ Finnish Meteorological Institute, Climate Change Unit, P.O. Box 503, FI-00101 Helsinki Finland, email: gerrit.leeuw@fmi.fi

⁽²⁾ University of Helsinki, Department of Physics, P.O. Box 64, Helsinki, FIN- 00014, Finland

⁽³⁾ TNO-B&O, Postbus 80015, 3508 TA Utrecht, The Netherlands

⁽⁴⁾ University of Bremen, The Institute of Environmental Physics, Postfach 33 04 40 D-28359 Bremen, Germany

⁽⁵⁾ ARGOSS BV, PO Box 61, 8325 ZH Vollenhove, The Netherlands

⁽⁶⁾ European Space Agency, Wave Interaction & Propagation Section, PB 299, 2200 AG Noordwijk, The Netherlands

ABSTRACT

The AMARSI project aims at the development and validation of aerosol retrieval algorithms over ocean. One algorithm will be developed for application with data from the Multi Spectral Imager (MSI) on EarthCARE. A second algorithm will be developed using the combined information from AATSR and MERIS, for application to similar instruments on Sentinel-3, i.e. the Sea and Land Surface Temperature Imager (SLTS) and the Ocean and Land Colour Instrument (OLCI), respectively. A forward model has been developed based on SCIATRAN to simulate the top-of-atmosphere signal over clear sky ocean scenes.

1. INTRODUCTION

The impact of aerosols on the Earth's radiative budget is a matter of increasing concern. Uncertainties remain when trying to quantify their net impact. Aerosols have both direct radiative effects, through scattering and absorption of incoming solar radiation, and indirect radiative effects (e.g.: through their influence on cloud physical properties). It is one of the mission objectives of the future EarthCARE mission to better understand the interactions between aerosols and clouds and their impact on the radiative budget of the planet. Two instruments onboard the EarthCARE platform will provide aerosol information: the ATmospheric backscatter LIDar (ATLID) and the Multi-Spectral Imager (MSI) (Earthcare SRD).

There are quite a number of currently flying multi-spectral imagers providing similar measurements to what is anticipated from the MSI, i.e., aerosol optical properties over ocean, in clear sky conditions. Algorithms for the retrieval of aerosol optical thickness and Ångström exponent have been developed for multispectral imagers such as TOMS, AVHRR, SeaWiFS, (A)ATSR, MODIS, MISR, Polder, MERIS, OMI and GOME-2 (all polar orbiting) as well as MSG-SEVIRI and GOES (geo-stationary). (A)ATSR, Polder and MISR offer two or more viewing angles, which

allows for better dealing with the perturbing effect of surface reflectance, and POLDER offers polarization which allows for better aerosol characterization (non-spherical particles). Because these features are not available for MSI, they cannot be used in the actual retrieval for Earthcare addressed in AMARSI. However, it is important to include directional effects and polarization in the forward model that will be developed in the AMARSI project to simulate the reflected radiation at the top of the atmosphere (TOA). In the retrieval step the TOA reflected radiation is compared with the measured TOA radiation to determine the aerosol properties from the MSI signal.

The retrieval of surface reflectance from space, using multi-spectral imagers, is of prime interest to many remote sensing users because it is a key parameter to the exploitation of surface bio-geo-physical parameter retrieval. Surface reflectance retrieval is generally only possible once the atmospheric effects have been accounted for in the (TOA) measurements. Aerosols are variable temporally, spatially, in their vertical distribution, in their size distribution and their composition. Consequently, the calculated aerosol effects on the measured TOA signal are as good as the information on the occurrence of aerosols. Often this information is obtained from climatologies whereas the actual properties may be significantly different. Hence a number of possible choices are usually offered to describe the TOA radiation and the one best representing the measurements is selected by the retrieval algorithm. This requires a comprehensive understanding of the radiative processes, the aerosol properties and interactions with gases and with the underlying surface. At instrument level, high signal-to-noise ratios and an accurate absolute calibration are required to effectively retrieve aerosol properties and subsequently correct for their effects.

The process of atmospheric correction and aerosol optical properties retrieval, over ocean, in clear sky condition is a prerequisite to derive ocean colour. Not

surprisingly, a number of current and past missions deploying ocean colour multi-spectral imagers also share aerosol monitoring objectives (e.g. AVHRR, SeaWiFs, MODIS, MERIS).

Likewise, ATSR was developed to measure surface temperature. However, taking advantage of the single and dual view algorithms, the ATSR-2 instrument was used for aerosol retrieval over ocean [1,2,3] and over land [3, 4,5,]. In fact, the feasibility to retrieve aerosol properties over land was for the first time demonstrated with ATSR-2 data [4].

The Sentinel-3 (S-3) platform will fly the Ocean and Land Colour Instrument (OLCI) and the Sea and Land Surface Temperature instrument (SLST) which are very similar to MERIS and AATSR, respectively.

In this contribution we present the AMARSI project, aimed at the retrieval of aerosol properties over open ocean (case 1 waters), using data from MSI and from the exploitation of the synergy between MERIS and AATSR.

2. OBJECTIVES

The AMARSI objectives are:

- Develop and verify a forward model capable of simulating the top-of-atmosphere signal over clear sky ocean scenes, in the presence of aerosols
- Develop and validate an aerosol retrieval algorithm for the MSI onboard EarthCARE
- Develop and validate an aerosol retrieval algorithm using both MERIS and AATSR data as input
- Provide recommendations for the EarthCARE and S-3 mission both at system level and algorithm level.

The aerosol retrieval algorithm for AATSR/MERIS will be implemented in the BEAM software package.

3. APPROACH

The approach to reach these objectives consists of the following elements. A literature study has been conducted to provide an overview of knowledge acquired in previous studies and to consolidate the requirements for the AMARSI study. Next a vector radiative transfer model was developed, based on SCIATRAN, which is briefly described below. This forward model is used to simulate the radiation at the top of the atmosphere, with user-selected input

atmospheric data, in particular aerosol models, over surfaces with a given reflectance. This forward model is used to create a series of look-up tables (LUT) for a range of sun-satellite geometries and aerosol models which are used in the retrieval step for comparison with the observed TOA radiation. By minimization of the observed and computed TOA radiation, using all available and suitable wavelengths, the best-fitting aerosol model is selected to represent the aerosol optical depth (AOD). The aerosol models used are selected from an aerosol climatology derived from AERONET [7] observations (cf. [8]).

The retrieval algorithms are developed for MSI and for the combined AATSR/MERIS observations, as described below.

4. FORWARD MODELING: SCIATRAN

SCIATRAN is the radiative transfer solver aimed at the solution of a wide range of direct and inverse problems of atmospheric optics. The earlier version of the code is described by [9]. During last years the software package SCIATRAN was upgraded to the full vector mode and now it is capable to calculate not only intensity but also the polarization characteristics of solar light in the terrestrial atmosphere. In this paper the recent version of SCIATRAN including the radiative transfer solver and relevant databases is briefly described. We compare SCIATRAN calculations with other published results and prepare benchmark tables, which can be of help for the users of the code and also for the developers of new radiative transfer codes aimed at the solution of the vector radiative transfer equation for realistic vertically inhomogeneous atmospheres with underlying surfaces having arbitrary angular and spectrally dependent reflective properties.

4.1. Radiative transfer solver

The radiative and polarization characteristics of light in the terrestrial atmosphere are usually described in the framework of the radiative transfer theory [10]. In particular, the following vector radiative transfer equation (VRTE) (with corresponding boundary conditions) is used to describe the Stokes $\vec{S}(\vec{r}, \vec{n})$ vector of multiply scattered light at any point with the radius – vector \vec{r} in the direction specified by the vector \vec{n} , see Eq. 1 :

$$\nabla_{\vec{r}} \vec{S}(\vec{r}, \vec{n}) = -k_{ext}(\vec{r}) \vec{S}(\vec{r}, \vec{n}) + \frac{k_{sca}(\vec{r})}{4\pi} \int_{\vec{n}'} \hat{P}(\vec{r}, \vec{n}, \vec{n}') \vec{S}(\vec{r}, \vec{n}') d\vec{n}' + \vec{B}_0(\vec{r}, \vec{n}) \quad (1)$$

Here k_{ext} is the extinction coefficient, k_{sca} is the scattering coefficient, and $\hat{P}(\vec{r}, \vec{n}, \vec{n}')$ is the phase matrix, which describes the transformation of the incoming Stokes vector $\vec{S}(\vec{n}', \vec{r})$ at the point with the radius - vector \vec{r} from the direction \vec{n}' to the direction \vec{n} in which observations are performed. The vector $B_0(\vec{r}, \vec{n})$ describes the internal (e.g., thermal) radiation sources. The components of the Stokes vector \vec{S} are defined as follows: $I = I_l + I_r$, $Q = I_r - I_l$, $U = E_l E_r^* + E_r E_l^*$, $V = i(E_l E_r^* - E_r E_l^*)$, where we neglected a common multiplier and $I_l = E_l E_l^*$ is the scattered light intensity in the meridional plane. This plane contains the normal to a light scattering slab and the direction of observation. The value of $I_r = E_r E_r^*$ gives the scattered light intensity in the plane perpendicular to the meridional plane. E_l and E_r are components of the electric vector of the scattered wave defined relative to the meridional plane in the same way as I_l, I_r [11]. In writing Eq. 1 we assumed that the medium is symmetric and isotropic. Therefore, the extinction matrix \hat{k}_{ext} is reduced to the extinction coefficient k_{ext} . Also the time-dependent effects (e.g., relevant to studies of laser pulses in atmosphere) and incoherent scattering (e.g., Raman, fluorescence) have been neglected.

4.2. Databases

Both for the solution of forward and inverse problems using SCIATRAN, the models of input atmospheric ($\omega_0(z) = k_{sca}(z)/k_{ext}(z)$, $\hat{P}(z, \vartheta, \varphi, \vartheta', \varphi')$) and surface ($\hat{R}_s(\tau_0, \vartheta, \varphi, \vartheta', \varphi')$) parameters are needed. The models used in SCIATRAN databases are described in this section.

4.2.1. Atmospheric parameters

The atmospheric scattering is presented as a linear mixture of different scattering processes, including molecular scattering, scattering by aerosol particles and scattering by cloud droplets. Absorption processes are also included in the considered radiative transfer problems including absorption of light by trace gases and liquid or solid particles suspended in atmosphere. Absorption cross sections of gases (dependent on pressure and temperature) are taken from HITRAN. Aerosol models are taken from LOWTRAN and also from the World Meteorological Organization standard models, which include dust particles, soot, oceanic

aerosols, and water soluble aerosols. Local optical characteristics of particles (including phase matrices) have been pre-calculated in the spectral range 0.24-20 μm and stored in special databases, which are ready to be used in SCIATRAN simulations in the broad spectral range from the UV to the thermal infrared.

4.2.2. Oceanic surface reflectance

SCIATRAN has a capability to perform calculations of the top-of-atmosphere reflectance for a spectral Lambertian albedo of the underlying surface. Also the calculations with account for the reflection function (RF) of an underlying surface are possible. In particular, in the case of ocean, the RF, which is equal to $\pi I / F \mu_0$ (F is the incident flux density), μ_0 is the cosine of the solar zenith angle, I is the reflected light intensity) is composed of three terms with the possibility to vary the contribution of each term depending on the user:

- Fresnel reflection (with account for light polarization);
- water-leaving radiation (Gordon approximation in the scalar case is used);
- the foam spectral reflectance (scalar approximation).

So we use the expression given by Eq. 2 for the total reflection function of the oceanic surface:

$$\mathfrak{R} = sR_f + (1-s)(R_{WL} + R_{FR}), \quad (2)$$

where R_f is the foam reflectance, R_{WL} is the water leaving radiation contribution, R_{FR} is the first element of the corresponding surface reflection matrix in the framework of the Cox-Munk approximation and s is the foam fraction parameterized as follows: $s = \zeta v^\nu$, where $\zeta = 2.95 \times 10^{-6}$, $\nu = 3.52$, and v is the wind speed (ms^{-1}).

4.2.3. Fresnel reflection

The amplitude of the Fresnel reflection coefficients are given by Eq. 3:

$$r_1 = \frac{mc_1 - c_2}{mc_1 + c_2}, \quad r_2 = \frac{c_1 - mc_2}{c_1 + mc_2} \quad (3)$$

where $c_1 = \cos \vartheta_0$, $c_2 = \sqrt{1 - (1 - c_1^2)/m^2}$, ϑ_0 is incidence angle and m is the refractive index of water and it is assumed that the refractive index of air is equal to 1.0. For most applications, one can neglect the imaginary part of m in calculations of reflection coefficients. If the ocean surface is flat, the reflection function can be written as (Eq 4):

$$R_F = \frac{\pi}{\mu'} r_f(\mu') \delta(\mu - \mu') \delta(\varphi - \varphi'), \quad (4)$$

where μ' is the cosine of the incident angle and φ' is the azimuth of the incident light, and

$$r_f = \frac{1}{2} \left[|r_1|^2 + |r_2|^2 \right]. \quad (5)$$

Due to existence of waves, the reflection function must be modified. Usually the Cox-Munk approximation for the RF (Eqs. 6, 7) is used:

$$\hat{R}_{CM} = \hat{R}_F \cdot \frac{\pi W(\mathcal{G}_0, \mathcal{G}, \phi)}{4\mu_n \cos \mathcal{G}_0 \cos \mathcal{G}}, \quad (6)$$

$$\mu_n = \frac{\cos \mathcal{G}_0 + \cos \mathcal{G}}{\sqrt{2(1 - \cos \theta)}}, \quad (7)$$

where \hat{R}_F is the Fresnel reflection matrix of the oceanic surface, $\mu_n = \frac{\cos \mathcal{G}_0 + \cos \mathcal{G}}{\sqrt{2(1 - \cos \theta)}}$,

$\cos \theta = -\cos \mathcal{G}_0 \cos \mathcal{G} + \sin \mathcal{G}_0 \sin \mathcal{G} \cos \phi$ is the scattering angle and $W(\mathcal{G}_0, \mathcal{G}, \phi)$ is the so-called wave slope Probability Distribution Function (PDF). The value of R_{FR} coincides with the first element of the matrix \hat{R}_{CM} . The matrix \hat{R}_F is calculated in SCIATRAN using the freely available code ocean.phase.f, located at <http://www.giss.nasa.gov/~cirmim/brf> (see also the complete description of corresponding equations in the paper prepared by [11] Mishchenko and Travis (1997)). There are different approaches to calculate the PDF. In particular, in SCIATRAN the Gram-Charlier PDF (Eq. 8) is used [12]:

$$W(\mathcal{G}_0, \mathcal{G}, \phi) = \frac{\exp(-(A^2 + B^2)/2)}{2\pi\sigma_c\sigma_u} \left\{ 1 - \frac{c_{21}B}{2}(A^2 - 1) - \frac{c_{03}B}{6}(B^2 - 3) + \frac{c_{40}}{24}(A^4 - 6A^2 + 3) + \frac{c_{22}}{4}(A^2 - 1)(B^2 - 1) + \frac{c_{04}}{24}(B^4 - 6B^2 + 3) \right\}, \quad (8)$$

where:

$$A = \frac{z_x \sin \phi_w - z_y \cos \phi_w}{\sigma_c}, \quad (9)$$

$$B = \frac{z_x \cos \phi_w + z_y \sin \phi_w}{\sigma_u}, \quad (10)$$

$$z_x = -\frac{\sin \mathcal{G} \cos \phi - \sin \mathcal{G}_0}{\cos \mathcal{G}_0 + \cos \mathcal{G}}, \quad (11)$$

$$z_y = -\frac{\sin \mathcal{G} \sin \phi}{\cos \mathcal{G}_0 + \cos \mathcal{G}}, \quad (12)$$

and ϕ_w is the azimuth of upwind direction relative to the direction of solar light, σ_c is the cross wind component of the mean square slope and σ_u is the corresponding upwind component. The coefficients c_{ij} are calculated using [12] $c_{04}=0.23$; $c_{22}=0.12$; $c_{03}=0.04-0.033v$; $c_{21}=0.01-0.0086v$.

4.2.4 Water-leaving radiation

The water leaving radiance is calculated using the modified Gordon approximation. It follows in the framework of this approximation for the reflection function [13] (Eq. 13):

$$R_{WL} = A \frac{\beta(\theta_s)}{k_{abs}(\lambda)}, \quad (13)$$

where

$\theta_s = \arccos(-\cos \theta_0 \cos \theta + \sin \theta_0 \sin \theta \cos \phi)$ is the scattering angle, k_{abs} is the absorption coefficient of water, $\beta(\theta) = 4\pi k_{sca} P(\theta)$ is the volume scattering coefficient of water and

$$A = \frac{\pi}{\mu + \mu_0}, \quad (14)$$

where we neglected small differences of the forward scattering fraction at the ocean surface from the value equal to one. The equation for A must be modified to take into account the interface air-water. In particular A must be multiplied by the factor Φ (Eq. 15)

$$\Phi = (1 - r_{aw}(\mathcal{G}_0))(1 - r_{wa}(\mathcal{G}^*))m^{-2}, \quad (15)$$

where m is the water refractive index, \mathcal{G}^* is the angle of incidence on the water – air interface from water and r_{aw} and r_{wa} are given by Eqs. 16 and 17:

$$r_{aw}(\mathcal{G}_0) = \frac{1}{\pi} \int_0^{2\pi} d\varphi \int_0^{\pi/2} d\mathcal{G} \cos \mathcal{G} \sin \mathcal{G} R_{CM}(\mathcal{G}_0, \mathcal{G}, \varphi) \quad (16)$$

$$r_{wa}(\mathcal{G}) = \frac{1}{\pi} \int_0^{2\pi} d\varphi \int_0^{\pi/2} d\mathcal{G}' \cos \mathcal{G}' \sin \mathcal{G}' R_{wa}(\mathcal{G}^*, \mathcal{G}', \varphi) \quad (17)$$

Here R_{wa} is similar to R_{CM} but for the illumination of the surface from below. For the forward modeling, one needs to have the spectral coefficients $\beta_\lambda(\theta)$. They are modeled by Eq. 18:

$$\beta_\lambda(\theta) = \beta_{w\lambda}(\theta) + \beta_{p\lambda}(\theta), \quad (18)$$

where $\beta_{w\lambda}(\theta)$ is the volume scattering coefficient of the pure water and $\beta_{p\lambda}(\theta)$ is the same coefficient but for the particulate matter always present even in remote oceanic areas as a result of biological activity or the long-range transport and deposition of aerosols (e.g., desert dust) from continents. There are various

models to describe the function $\beta_{p\lambda}(\theta)$. In particular, [14] proposed the model described by Eq. 19:

$$\beta_{p\lambda}(\theta) = c_s \beta_s(\theta) \left(\frac{550}{\lambda} \right)^{1.7} + c_l \beta_l(\theta) \left(\frac{550}{\lambda} \right)^{0.3} \quad (19)$$

Here c_s is the concentration of the fine particulate matter (PM) fraction in the oceanic water and c_l is the concentration of the coarse PM fraction (in cm^3/m^3), λ is the wavelength measured in nm and functions $\beta_s(\theta)$, $\beta_l(\theta)$ are usually given in the tabular form [14].

The absorption coefficient $k_{abs}(\lambda)$ is modeled by [15] Eq. 20:

$$k_{abs}(\lambda) = \alpha_w(\lambda) + 0.06 p(\lambda) c^{0.65} + 0.2(\alpha_w(\lambda_0) + 0.06 c^{0.65}) \exp(-0.014(\lambda - \lambda_0)), \quad (20)$$

at wavelengths smaller than 700nm. Here c is the chlorophyll concentration (in $mg\ m^{-3}$, usually in the range 0.03-3 $mg\ m^{-3}$), λ is the wavelength (in nm) and $\lambda_0 = 440nm$. The function $p(\lambda)$ and the pure water absorption coefficient $\alpha_w(\lambda)$ are usually given in the tabular form [15].

4.2.5. Reflection of light from whitecaps

The whitecaps reflectance R_f in the spectral range 400-700nm is modeled [13] by Eq. 21:

$$R_f = \exp(-\sqrt{Y k_{abs}(\lambda)}), \quad (21)$$

where $Y = 0.0171$ and k_{abs} (in m^{-1}) is given in the previous section. The value of Y depends on the wind speed and can be varied in the framework of SCIATRAN.

5. AEROSOL RETRIEVAL USING MSI DATA

The aerosol retrieval algorithm for the EarthCARE Multi-Spectral Imager (MSI) is intended to provide aerosol information complementary to that from the

other EarthCARE instruments: the space-borne LIDAR – ATLID, the Cloud-Precipitation-Radar (CPR) and the Broadband Radiometer (BBR). With ATLID and CPR being profiling instruments, MSI will provide information on the column-integrated conditions in the vicinity of the LIDAR and radar beams as well for cloud free conditions. For the case of cloud free conditions the aerosol optical thickness (AOD) is required.

The MSI instrument is a nadir looking pushbroom imager with three cameras for the VIS, NIR and TIR regions. It has in total 7 channels, 4 channels are in VIS and NIR, which will be used for the aerosol retrieval approach: 0.659, 0.865, 1.610 and 2.200 μm center wavelength and 10 nm band width in the VIS and 15 nm in the NIR, the other 3 channels are in the TIR: 8.8, 10.8 and 12.0 μm . The MSI instrument has a swath width of 150 km, asymmetrically tilted from sun and a spatial resolution of 0.5 km.

For the retrieval of aerosol properties from MSI, an existing algorithm will be modified for the conditions of the MSI instrument. Below we describe the algorithm approach, and its testing and validation.

5.1. Main features of the AOD retrieval

The algorithm is based on the determination of aerosol reflectance ρ_{Aer} from the measured top-of-atmosphere

reflectance ρ_{TOA} , by correcting Rayleigh path reflectance ρ_{Ray} and surface conditions A_{Surf} , described

$$\rho_{Aer}(z_0, z_S, \phi, p_{Aer}(\theta), \omega_0, 0) = \rho_{TOA}(z_0, z_S, \phi) - \rho_{Ray}(z_0, z_S, \phi, p, 0) - \frac{t_{tot}(z_0)t_{tot}(z_S)A_{Surf}}{1 - A_{Surf}r_{hem}(\delta_{tot}, g)} \quad (22)$$

For the surface term the following first assessments are made: a) the water leaving reflectance is 0, b) surface reflection is modelled, using Cox-Munk reflection, c) no whitecaps are considered. It is planned to consider wind speed dependence for b) and c).

The AOD will be obtained by applying look-up-tables, giving relationships between the aerosol reflectance ρ_{Aer} and the AOD, δ_{Aer} for each channel used. The LUT are used as air mass corrected relations in form of Eq. 23:

$$\delta_{Aer} = f\left(\rho_{Aer} \cdot \frac{M_1 + M_2}{M_1 \cdot M_2}\right), \quad (23)$$

where M1 and M2 are the air mass factors for the solar illumination and satellite viewing directions respectively. An example of air mass normalized LUT for 0.66 μm (MSI channel 1) is presented in Figure 1.

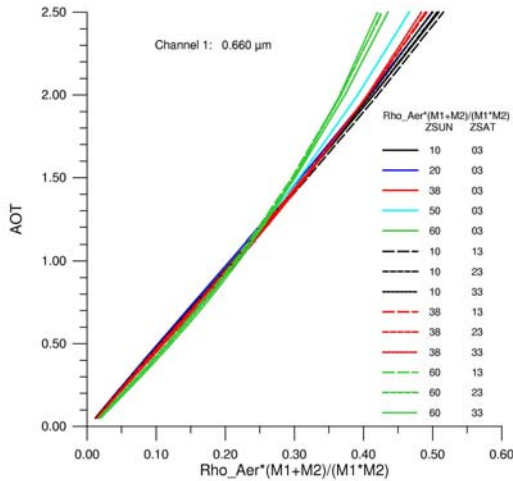


Figure 1: Relationships between the air mass normalized aerosol reflectance and the AOD for the wavelength 0.66 μm obtained from radiative transfer modelling with a given aerosol type.

5.2. First Tests of the Algorithm

First tests have been started with this approach. Data from other instruments with the MSI wavelengths have been used for this purpose. Figure 2 presents an example of the AOD for 0.665 μm , obtained from MERIS channels 7 (0.665 μm) and 13 (0.865 μm). The

by Eq. 22:

difference between the retrieved AOD at 0.665 μm (AOD = 0.073) and the AERONET measurements of the Helgoland site (AOD = 0.0661) in the North Sea is about 0.01 and looks promising.

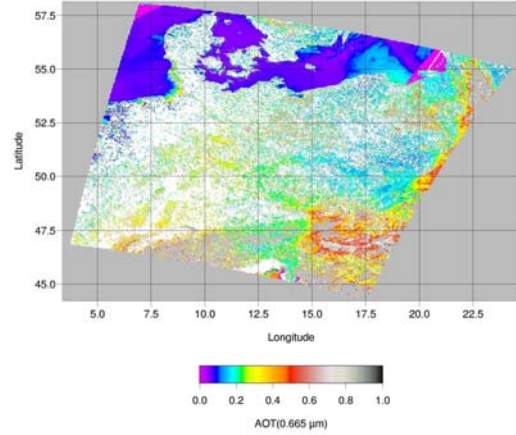


Figure 2: First test of the AOD retrieval, using channels 7 (0.665 μm) and 13 (0.865 μm) of the MERIS instrument, corresponding to channels 1 and 2 of MSI. (MERIS L1 data of 12.06.2006)

Tests with data, having all 4 MSI VIS and NIR channels, are scheduled. For this purpose it is planned to extract the corresponding channels from MODIS L1 data.

6. AEROSOL RETRIEVAL USING AATSR AND MERIS DATA

The aerosol retrieval algorithm for the combined AATSR and MERIS data will build on the existing algorithms for these instruments, but advantage will be taken of the extended range of wavelengths, from the UV to the thermal infrared (TIR). The AATSR algorithm follows from the ATSR-2 algorithm [1] which uses either the nadir or the forward view, with consistent results. It has an automated cloud detection procedure consisting of four standard cloud detection tests as described in [16]. These tests are applied to individual pixels and are classified as clear if and only if all tests indicate the no cloud is detected. They are based on the evaluation of histograms of either brightness temperature or reflectance. To determine whether a pixel is cloud contaminated, thresholds are set which depend on the surface properties and the sun-satellite geometry. The thresholds are determined for each individual frame of 512 x 512 pixels, in two steps.

First, a Fast Fourier Transform low-pass filter is applied to smooth the data. Then the extrema (maximum, minimum and inflexion points) of the smooth histogram are computed by applying a modified Lagrange interpolation, and from this set of extrema the thresholds for each test are determined.

For cloud free pixels, the effect of the ocean surface on the TOA radiation is corrected for by utilizing a model that accounts for chlorophyll, waves and water reflection. This leaves the path reflectance from which the AOD at wavelengths in the visible and near infrared are determined using LUTs as described in section 3. The LUTs will be created using SCIATRAN. Both the forward and nadir views will be used to check for internal consistency.

At this point, the experimental data base is extended with the MERIS wavelengths to determine the AOD in the UV and, possibly, at intermediate wavelengths to optimize the retrieval accuracy by using the appropriate information over a wide range of wavelengths. The major problem here will be to account for the water leaving radiance at the shorter wavelengths. To determine the aerosol parameters that can be independently determined, a principal component analysis has been undertaken.

7. VALIDATION APPROACH

For validation of the retrieval results, use will be made of the AERONET data at coastal and island stations, selected for their representativeness for open ocean. In particular, the Marine Aerosol Network (MAN), is an interesting source of information, as an alternative to observations from islands. Since 2004, hand-held sun photometers have been deployed periodically on ships of opportunity and research vessels to monitor aerosol properties over the World Oceans. An overview of MAN, MERIS and AATSR match-ups has been prepared for cloud-free situations.

8. CONCLUSIONS

An overview has been presented of the AMARSI project. Several components have been completed, i.e. the literature review and the SCIATRAN forward model has been delivered. The MSI algorithm will be ready for initial testing and evaluation in September 2008. The combined AATSR/MERIS algorithm is being developed for initial testing in early 2009. The final step is the implementation of both retrieval algorithms in the BEAM software package.

9. REFERENCES

1. Veefkind, J.P. & de Leeuw, G. (1998). A new algorithm to determine the spectral aerosol

optical depth from satellite radiometer measurements. *Journal of Aerosol Sciences*, **29**, 1237-1248.

2. Veefkind, J.P., de Leeuw, G., Durkee, P.A., Russell, P.B., Hobbs, P.V., & Livingston, J.M. (1999). Aerosol optical depth retrieval using ATSR-2 and AVHRR data during TARFOX. *Journal of Geophysical Research*, **104**, D2, 2253-2260.
3. Veefkind, J.P. (1999). Aerosol Satellite remote sensing, PhD dissertation, University of Utrecht, Utrecht, The Netherlands.
4. Veefkind, J.P., de Leeuw, G. & Durkee, P.A. (1998b). Retrieval of aerosol optical depth over land using two-angle view satellite radiometry during TARFOX. *Geophysical Research Letters*, **25**, 3135-3138.
5. Veefkind, J.P., de Leeuw, G., Stammes P., & Koелеmeijer, R.B.A. (2000). Regional distribution of aerosol over land derived from ATSR-2 and GOME. *Remote Sensing of Environment*, **74**, 377-386.
6. Mishchenko, M.I., & Travis L.D. (1997). Satellite retrieval of aerosol properties over the ocean using polarization as well as intensity of reflected sunlight, *J. Geophys. Res.*, **102**, 16989-17013.
7. Holben, B.N., Eck, T. F., Slutsker, I., Tanré, D., Buis, J. P., Setzer, A., Vermote, E., Reagan, J. A., Kaufman, Y. J., Nakajima, T., Lavenu, F., Jankowiak, I. & Smirnov, A. (1998). AERONET-A Federated Instrument Network and Data Archive for Aerosol Characterisation, *Remote Sensing of the Environment*, **66**, 1-16.
8. Levy, R.C., Remer, L.A., & Dubovik, O. (2007). Global aerosol optical properties and application to MODIS aerosol retrieval over land. *J. Geophys. Res.*, **112**, D13210, doi:10.1029/2006JD007815.
9. Rozanov, A. A., Rozanov V.V., Buchwitz M., Kokhanovsky A.A., & Burrows J.P. (2005). SCIATRAN 2.0-a new radiative transfer model for geophysical applications in the 175-2400 nm spectral range, *Adv. Space Res.*, **36**, 1015-1019.
10. Zege et al. (1991) *Image Transfer Through a Scattering Medium*, Berlin: Springer.
11. van de Hulst, H.C. (1980). *Multiple Light Scattering: Tables, Formulas and Applications*, N.Y.: Academic Press.
12. Cox, C. & W. Munk (1954). Measurement of the roughness of the sea surface from photographs of the suns glitter, *J. Opt. Society of America*, **44**, 838-850.
13. Kokhanovsky, A. A. (2004) *Light Scattering Media Optics: Problems and Solutions*, Berlin: Springer-Praxis.
14. Kopelevich, O. V. (1983) Small-parameter model of optical properties of seawater, in Ocean

- Optics, v.1, : *Physical ocean optics*, ed. A. S. Monin, Nauka, Moscow (in Russian), 208-234.
15. Morel A., & Maritorena S. (2001) Bio-optical properties of oceanic waters: a reappraisal, *J. Geophys. Res.*, **C106**, 7163-7180.
 16. Curier, L., de Leeuw G., Kolmonen P., Sundström A.-M., Sochageva L., & Bennouna Y. (2009). Aerosol retrieval over land using the ATSR dual-view algorithm. In: A. A. Kokhanovsky and G. de Leeuw (Eds.), *Satellite Aerosol Remote Sensing Over Land*, Springer-Praxis (Berlin)